JOURNAL OF COMPUTATIONAL PHYSICS 47, 179–198 (1982)

The Calculation of Eigenvalues for the Stationary Perturbation of Poiseuille Flow

J. S. BRAMLEY* AND S. C. R. DENNIS

Department of Applied Mathematics, University of Western Ontario, London, Ontario, Canada

Received October 14, 1981

The problem considered is that of two-dimensional viscous flow in a straight channel. The decay of a stationary perturbation from the Poiseuille flow in both the upstream and downstream directions is sought. A differential eigenvalue equation resembling the Orr–Sommerfeld equation is solved using a spectral method for values of the Reynolds number R between 0 and 2000. Although the decay downstream has received considerable previous attention, the situation upstream has not been studied in detail. It is found that for R greater than about 250, the upstream disturbances decay more rapidly by an order of magnitude greater than the downstream disturbances. The eigenfunctions are used to obtain an asymptotic solution for two-dimensional channel flow both upstream and downstream and comparison is made with a previous numerical solution for flow in a channel with a step change in width.

1. INTRODUCTION

Incompressible viscous flow in a channel has been the subject of many computational studies. Various combinations of channel geometry can be considered, but most of the problems of this type assume Poiseuille flow far down a straight channel or pipe as either the entry flow or the exit flow or both. In the present work, attention is confined to the two-dimensional problem of flow in a straight channel; an asymptotic solution of the Navier–Stokes equations in a region where the flow is slightly perturbed from the Poiseuille flow is considered. The equations are linearised on the assumption of a small stationary disturbance from the parallel flow. This leads to a differential eigenvalue equation for the decay of a stationary perturbation very similar to the Orr–Sommerfeld equation. The problem of determining the asymptotic decay downstream has previously been attempted by, amongst others, Gillis and Brandt [4] and Wilson [12]. The problem of entry flow to a channel under various entry conditions has been investigated by Van Dyke [9] and Wilson [13], although perturbations from Poiseuille flow upstream were not specifically considered. In cases where they are applicable, perturbations to the Poiseuille flow can be used as asymptotic boundary conditions for flow into or out of a channel, thus reducing the domain of computation and cutting down the computational time.

* Permanent address: Department of Mathematics, University of Strathclyde, Glasgow, United Kingdom.

0021-9991/82/080179-20$02.00/0

581/47/2-2

It is possible to solve the differential eigenvalue equation by two very different methods, namely, an initial-value type method or a spectral method. The dependent variable of the ordinary differential equation is expressed as an expansion of Chebyshev polynomials resulting in a generalised algebraic eigenvalue problem, which is solved by using the QR matrix eigenvalue algorithm. The method employed here is analogous to that used by Orszag [8] in his treatment of the Orr–Sommerfeld stability equation.

An attempt is made to employ the eigensolutions to describe the asymptotic behaviour of the flow both upstream and downstream in a channel in a specific example. To this end we compare various asymptotic formulations derived from the theory with the data of Dennis and Smith [2] obtained in solving the problem of flow in a channel with a step. The agreement is excellent upstream but downstream it is more tentative.

2. Equations

Following Wilson [12], the nondimensional stream function $\psi(x, y)$ satisfies the equation

$$\left(\frac{\partial\psi}{\partial y}\frac{\partial}{\partial x}-\frac{\partial\psi}{\partial x}\frac{\partial}{\partial y}\right)\nabla^2\psi=\frac{1}{R}\nabla^4\psi, \tag{2.1}$$

where x is the (dimensionless) downstream coordinate, y is the (dimensionless) transverse coordinate, and $R = aU/v$ is the Reynolds number, with a half the channel width and Ua the volumetric flow rate of the Poiseuille flow over half the channel width. If the quantities u and v are, respectively, the velocity components in the x and y directions, then they are related to ψ by

$$u = \partial\psi/\partial y, \qquad v = -\partial\psi/\partial x. \tag{2.2}$$

The origin is at the centre of the channel and the boundary conditions on the walls $y = \pm 1$ are

$$\psi(x, \pm 1) = \pm 1, \qquad \partial\psi/\partial y = 0 \qquad \text{when} \quad y = \pm 1. \tag{2.3}$$

The velocity far upstream approaches the parabolic profile and so

$$\psi \to \tfrac{1}{2}(3y - y^3), \qquad \partial\psi/\partial x \to 0 \qquad \text{as} \quad x \to \pm\infty. \tag{2.4}$$

We now look for a perturbation solution where

$$\psi(x, y) = \tfrac{1}{2}(3y - y^3) + \varepsilon\phi(y)\exp(-\alpha x), \tag{2.5}$$

where ε is small. Substituting (2.5) in (2.1) and neglecting squares of ε leads to

$$\phi'^v + 2\alpha^2\phi'' + \alpha^4\phi + \alpha R[\tfrac{3}{2}(1 - y^2)(\phi'' + \alpha^2\phi) + 3\phi] = 0, \tag{2.6}$$

with boundary conditions

$$\phi(\pm 1) = \phi'(\pm 1) = 0. \tag{2.7}$$

Wilson [12] pointed out that the above equation is similar to the Orr–Sommerfeld equation. The main difference is that in the present equation, α is an eigenvalue, not a prescribed wave number; the equation is nonlinear in α, which in general will be complex. It is readily shown that, if α is an eigenvalue, so is α^* (the complex conjugate); the eigenfunction is ϕ^*. The complex eigenvalues are in conjugate pairs but for simplicity only one of the pair will be given in the numerical results, the one with positive imaginary part. We are interested only in decaying modes, since growing modes cannot satisfy the necessary conditions as $x \to \pm\infty$. The eigenvalues with positive real part have associated modes which decay as $x \to +\infty$ while those with negative real part are associated with modes which decay as $x \to -\infty$. It will be shown later that the results in these two cases are very different. The reason for considering eigenvalues with both positive and negative real parts is that the physical problems, in which the eigenfunctions might be used as asymptotic solutions, could involve flow out of channel or entry into a channel. The eigenfunctions will either be odd or even functions of y and the terms odd and even will be applied to the eigenvalues themselves. There is in fact an infinite sequence of eigenvalues here for each fixed R, which may be ordered by the magnitude of the real part. The proportion of real eigenvalues tends to increase with R. We only obtain a finite number of eigenvalues because the Chebyshev series used to approximate the solutions is terminated after a finite number of terms.

3. The Chebyshev Series Expansion

Orszag [8], in his treatment of the Orr–Sommerfeld equation, discussed the advantages of Chebyshev polynomials relative to other sets of orthogonal polynomials. In particular, he showed that if the coefficients of a linear differential equation are infinitely differentiable, the approximation obtained is of infinite order in the sense that errors decrease more rapidly than any power of $1/N$ as $N \to \infty$, where N is the number of Chebyshev polynomials used in the approximation. We therefore use Chebyshev polynomials to obtain a numerical solution of (2.6), subject to boundary conditions (2.7). The required properties of Chebyshev polynomials are outlined below and further details may be obtained from Orszag [8] or Fox and Parker [3].

The function $\phi(y)$ and the polynomial coefficients of (2.6) are infinitely differentiable in the interval $-1 \leqslant y \leqslant +1$. Let the Chebyshev expansion of $\phi(y)$ and its derivatives $d^q\phi/dy^q$ be

$$d^q\phi(y)/dy^q = \sum_{n=0}^{\infty} a_n^{(q)} T_n(y), \tag{3.1}$$

where $a_n^{(0)} \equiv a_n$ and $T_n(y)$ is the nth degree polynomial of the first kind, defined by

$$T_n(\cos\theta) = \cos n\theta, \tag{3.2}$$

for $n = 0, 1, 2, \ldots$. The properties of $T_n(y)$ are now used to express $a_n^{(q)}$ in terms of $a_n^{(q-1)}$. Two constants c_n and d_n are commonly used in the recurrence relations of Chebyshev polynomials and are given as

$$c_n = d_n = 0 \quad \text{for} \quad n < 0; \qquad c_0 = 2, \qquad d_0 = 1,$$
$$c_n = d_n = 1 \quad \text{for} \quad n > 0.$$

It can be shown that

$$c_n a_n^{(q)} = 2 \sum_{\substack{p=n+1 \\ p+n\equiv 1 \pmod 2}}^{\infty} p a_p^{(q-1)} \qquad (n \geqslant 0), \tag{3.3}$$

where $a \equiv b \pmod 2$ means that $a - b$ is divisible by 2. The second and fourth derivatives of ϕ are then given by

$$c_n a_n^{(2)} = \sum_{\substack{p=n+2 \\ p\equiv n \pmod 2}}^{\infty} p(p^2 - n^2)\, a_p \qquad (n \geqslant 0) \tag{3.4}$$

and

$$24 c_n a_n^{(4)} = \sum_{\substack{p=n+4 \\ p=n \pmod 2}}^{\infty} p(p^2 - n^2)[(p-n)^2 - 4][(p+n)^2 - 4]\, a_p \qquad (n \geqslant 0). \tag{3.5}$$

The coefficients of ϕ in (2.6) are constant except for the y^2 term, on which we use the property

$$4y^2 T_s(y) = T_{s-2}(y) + 2T_s(y) + T_{s+2}(y)$$

to find that the nth Chebyshev coefficient of $4y^2\phi(y)$ is

$$c_{n-2} a_{n-2} + (c_n + c_{n-1})\, a_n + a_{n+2} \qquad (n \geqslant 0). \tag{3.6}$$

A similar result holds for $4y^2\phi''(y)$ in terms of $a_n^{(2)}$ instead of a_n.

The above expansions are substituted into (2.6) and the coefficients of $T_n(y)$ may be equated by virtue of the orthogonality properties of the Chebyshev polynomial. This yields

$$a_n^{(4)} + 2\alpha^2 a_n^{(2)} + \alpha^4 a_n + \alpha R\left[\tfrac{3}{2} a_n^{(2)} - \tfrac{3}{8}\{c_{n-2} a_{n-2}^{(2)} + (c_n + c_{n-1})\, a_n^{(2)} + a_{n+2}^{(2)}\}\right.$$
$$\left. + (\tfrac{3}{2}\alpha^2 + 3)\, a_n - \tfrac{3}{8}\alpha^2\{c_{n-2} a_{n-2} + (c_n + c_{n-1})\, a_n + a_{n+2}\}\right] = 0. \tag{3.7}$$

The coefficients with superscripts 2 or 4 may be expressed in terms of the basic coefficients by using (3.4) or (3.5). We shall now restrict the summation and truncate the Chebyshev series at $T_N(y)$. This gives

$$\begin{aligned}
&\tfrac{1}{24} \sum_{\substack{p=n+4 \\ p=n(\mathrm{mod}\ 2)}}^{N} p(p^2-n^2)[(p-n)^2-4][(p+n)^2-4]\, a_p \\
&\quad + \sum_{\substack{p=n+2 \\ p=n(\mathrm{mod}\ 2)}}^{N} \{[2\alpha^2 + \tfrac{3}{8}\alpha R(4-c_n-c_{n-1})]\, p(p^2-n^2) - \tfrac{3}{8}\alpha R c_n\, p[p^2-(n+2)^2] \\
&\quad - \tfrac{3}{8}\alpha R d_{n-2}\, p[p^2-(n-2)^2]\}\, a_p - \tfrac{3}{2}\alpha R n(n-1)\, a_n + \{\alpha^4 + \tfrac{3}{2}R\alpha(\alpha^2-2)\}\, c_n a_n \\
&\quad - \tfrac{3}{8}\alpha^3 R[c_{n-2}a_{n-2} + c_n(c_n + c_{n-1})\, a_n + c_n a_{n+2}] = 0, \qquad (3.8)
\end{aligned}$$

for $0 \leqslant n \leqslant N$. If the expansion (3.1) and the properties $T_n(\pm 1) = (\pm 1)^n$, $T_n'(\pm 1) = (\pm 1)^{n-1}\, n^2$ are used on the boundary conditions $\phi(\pm 1) = \phi'(\pm 1) = 0$, we obtain

$$\sum_{n=0}^{N} a_n = 0, \qquad \sum_{n=0}^{N} (-1)^n a_n = 0, \qquad \sum_{n=0}^{N} n^2 a_n = 0 \qquad \text{and} \qquad \sum_{n=0}^{N} (-1)^{n-1} n^2 a_n = 0.$$

These boundary conditions will be more useful later if we add and subtract them to get

$$\sum_{\substack{n=0 \\ n\equiv 0(\mathrm{mod}\ 2)}}^{N} a_n = 0, \qquad \sum_{\substack{n=0 \\ n\equiv 0(\mathrm{mod}\ 2)}}^{N} n^2 a_n = 0 \qquad (3.9)$$

and

$$\sum_{\substack{n=1 \\ n\equiv 1(\mathrm{mod}\ 2)}}^{N} a_n = 0, \qquad \sum_{\substack{n=1 \\ n\equiv 1(\mathrm{mod}\ 2)}}^{N} n^2 a_n = 0. \qquad (3.10)$$

Equations (3.8)–(3.10) separate into two sets with no coupling between the odd subscript coefficients and the even subscript coefficients. To examine the even case, we replace N by $2M$, n by $2m$ and a_{2m} by $\hat{a}_m$. There are $M+1$ unknowns $\hat{a}_m$, $m = 0, 1, 2, \ldots, M$. If (3.8) were applied for $n = 0, 2, 4, \ldots, 2M$ together with the boundary conditions (3.9), we would have $M+3$ equations with $M+1$ unknowns with the only solution being the trivial one. Orszag [8] solved this over-specification by using Lanczos' tau method first described in [5]. The effect of this is not to use (3.8) for $m = M-1$ or M, and we thus have $M+1$ equations with $M+1$ unknowns. The odd solution is treated in a similar manner by restricting the number of equations used.

Although there are two distinct cases which have been designated as odd and even, they are treated in a similar manner to each other in the remainder of the paper. The problem is to find all the eigenvalues α for a given Reynolds number R. This causes

some difficulties because α occurs up to the power of four in (3.8). If we take α (real or complex) as a given parameter it is easier to treat R as the eigenvalue parameter and calculate all its values corresponding to this value of α because R appears linearly in (3.8). In Section 4 we describe this method of procedure and in Section 5 the general one of obtaining α for a given R.

4. The Inverse Problem

We first solve the eigenvalue problem by means of the inverse method, i.e., given α find all the eigenvalues R. This way the problem is much easier to solve and requires far less computer time. The results obtained are more useful than at first seems possible. We can use these results to check the results obtained by the method of Section 5 and to plot the eigenvalues R on a graph against α where it does not matter whether the results were obtained from the inverse problem or not.

Equations (3.8) with $M = 0, 1,..., M-2$ together with the boundary conditions (3.9) can be expressed in the form

$$(A - \lambda B)\mathbf{b} = 0, \tag{4.1}$$

where A, B are square matrices of dimension $M+1$, $\lambda = \alpha R$, and $\mathbf{b}$ is the eigenvector. Equation (4.1) is a generalised eigenvalue problem. The matrix B has zeros in the last two rows from the boundary conditions, and rank B = rank $A - 2$. This means that two of the eigenvalues are infinite and are ignored. In all the cases done, the rank of B is not decreased any more than described above. The matrices A and B are predominantly upper triangular.

The method used to solve (4.1) is described by Moler and Stewart [7] and is a generalisation of the standard QR algorithm. This routine is used as an ISML subroutine on a CYBER 73. It monitors the size of residuals, and in all cases the equations were well conditioned.

5. Calculation of All α for a Given R

It is desirable to be able to calculate all the eigenvalues (real and complex) for a particular Reynolds number. Equations (3.8) with $M = 0, 1,..., M-2$ together with the boundary conditions (3.9) can be expressed in the form

$$(\alpha^4 C_4 + \alpha^3 C_3 + \alpha^2 C_2 + \alpha C_1 + C_0)\mathbf{b} = 0, \tag{5.1}$$

where C_i $(i = 0, 1, 2, 3, 4)$ are square matrices of order $M+1$. This can be transformed to the generalised eigenvalue problem

$$(E - \alpha F)\mathbf{x} = 0, \tag{5.2}$$

where

$$E = \begin{bmatrix} C_3 & C_2 & C_1 & C_0 \\ I & 0 & 0 & 0 \\ 0 & I & 0 & 0 \\ 0 & 0 & I & 0 \end{bmatrix}, \qquad F = \begin{bmatrix} -C_4 & 0 & 0 & 0 \\ 0 & I & 0 & 0 \\ 0 & 0 & I & 0 \\ 0 & 0 & 0 & I \end{bmatrix},$$

and $\mathbf{x}^T = (\alpha^3\mathbf{b}^T, \alpha^2\mathbf{b}^T, \alpha\mathbf{b}^T, \mathbf{b}^T)$. There are two main differences from results in the previous section: E, F are square matrices of order $4M + 4$, and all but the top quarters of E and F are sparse. An attempt was made to solve the generalised eigenvalue problem (5.2) by the method of Moler and Stewart [7], as used in the previous section. With the increased matrices, rank F = rank $E - 8$, and there are now eight infinite eigenvalues which have to be ignored. There is also a large increase of computation time from the previous method, but a far more serious matter is that the residues become large for some of the eigenvalues with a serious loss of accuracy. By simple column operations it is now possible to reduce the size of matrices E and F to $4M - 4$, thus making the rank of E equal to the rank of F and eliminating the eight infinite eigenvalues. This reduced problem can now be solved using the method of Moler and Stewart [7], and the residues are small.

The revised matrix F is now nonsingular, upper triangular, and sparse. With the matrix E also having a large proportion of zero elements, the computation time can be reduced by solving the eigenvalue problem

$$(F^{-1}E - \alpha I)\mathbf{x} = 0. \tag{5.3}$$

The structures of the reduced matrices E and F are given in Figs. 1 and 2 for $M = 7$.

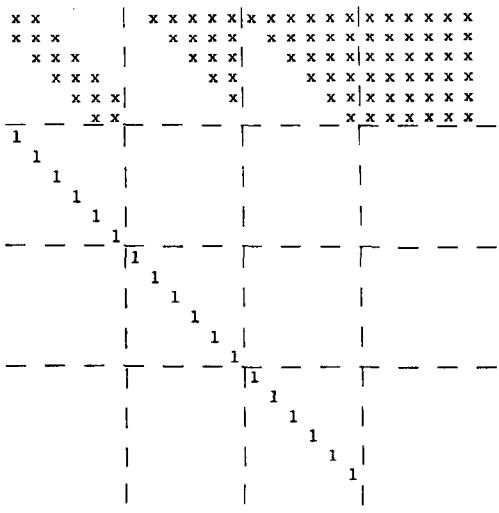

FIG. 1. Structure of matrix E after application of six column operations to make rank F = rank E.

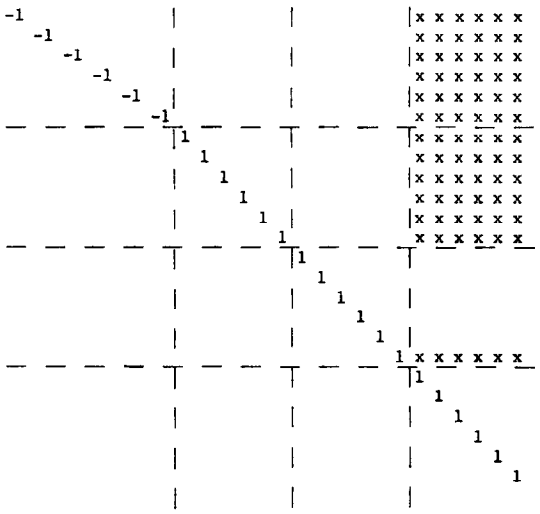

FIG. 2. Structure of matrix F after application of 16 column operations to make rank F = rank E.

The structures remain similar for M larger, the unit diagonals are shown, x denotes any real number, and all the rest of the elements are zero. The product $F^{-1}E$ is formed by simple row operations on E and F. The eigenvalue problem given by (5.3) is now solved using the QR algorithm of Wilkinson [10]. The size of the elements of the matrix $F^{-1}E$ can have a wide range, so the matrix $F^{-1}E$ is balanced using the method of Wilkinson and Reinsch [11] before using the QR algorithm. This is one more advantage of reducing the problem to find the eigenvalue of a single matrix.

6. NUMERICAL RESULTS

A large volume of numerical data is generated and we try to present the main results in as concise a way as possible. The results for real α are presented in graphical form for $R \leqslant 1000$. The majority of these results are obtained by solving the inverse problem as stated in Section 4. The value of M was varied, and $M = 16$ gave sufficiently accurate results. Random checks are made by using the full method of Section 5, and both sets of results were entirely in agreement with each other. Figures 3 and 4, respectively, give the first six positive odd and even eigenvalues. It will be seen that in both cases there are values of R below which there are no positive real eigenvalues. Gillis and Brandt [4] called the value of R below which there was no real positive eigenvalue R_{crit}. These authors only obtained one eigenvalue for the odd case, and that would correspond to the lowest curve of Fig. 3. The results of Gillis and Brandt agree with this curve with one notable exception: they calculated $R_{\text{crit}} = 8.461$ at $\alpha = 2.632$, whereas Fig. 3 suggests that $R_{\text{crit}} = 6.3$ at $\alpha = 6.0$. For $R = 6.0$, the full problem solution gives eigenvalues $\alpha = 8.39$, 9.63, and 10.94, which

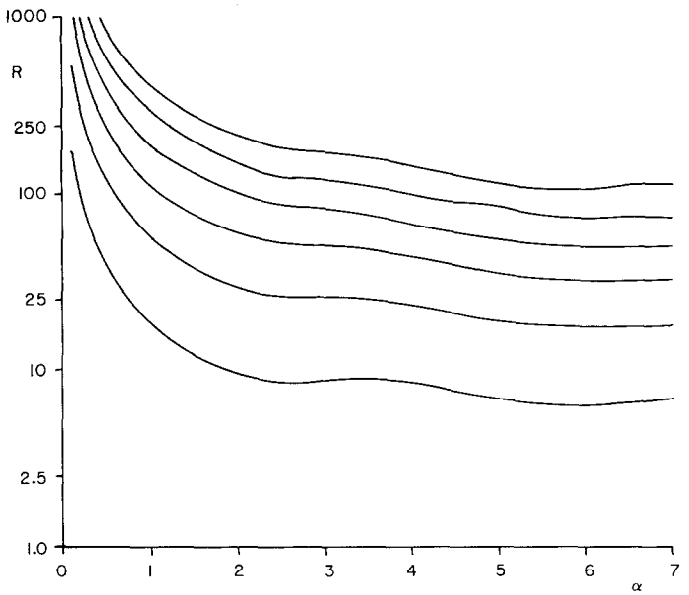

FIG. 3. Graph of positive real odd eigenvalues against Reynolds number.

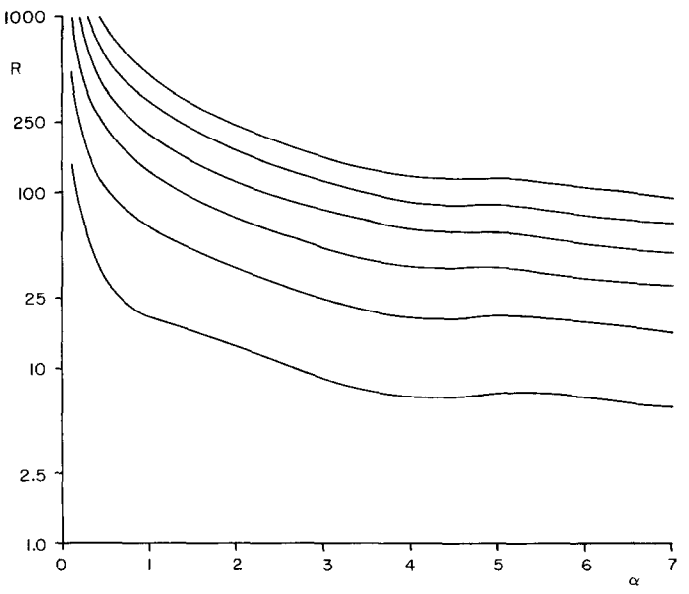

FIG. 4. Graph of positive real even eigenvalues against Reynolds number.

are all out of range of Fig. 3. It is easy to see why Gillis and Brandt derived the wrong value; they found a relative minimum but not the smallest relative minimum. The value R_{crit} is not really important, but taking into account both odd and even eigenvalues, there are no real positive eigenvalues for $R \leqslant 5.0$. In Figs. 3 and 4, undulations will be noticed as α increases. These undulations have been cross-checked using both methods. The undulations mean that the number of real eigenvalues does not decline monotonically as we reduce R. In the even eigenvalue case, when $R = 10$ we only have one positive eigenvalue $\alpha = 2.6737$, whereas when $R = 7$ we have eigenvalues $\alpha = 3.9525, 4.5121, 6.0627$, etc. In Figs. 3 and 4, it is impossible to suggest an asymptote as α becomes large, but the values of R at $\alpha = 7.0$ are very similar in the two cases.

As suggested in Section 2, we are also interested in the negative real eigenvalues which are given in Figs. 5 and 6 for the odd and even cases, respectively. In these cases as well, the curves are not always monotonically decreasing. There are values of R for which there are negative real eigenvalues but no positive ones. Note that the negative eigenvalues vary only slightly for R greater than 50, in marked contrast to the positive eigenvalues. We shall return to this point later. In Figs. 3–6, the curves at the right-hand side of the graphs are not tending to an asymptote. If the inverse problem is solved for α of larger modulus than in these figures, the values of R obtained do increase after a while. These results are not presented because our main interest is in eigenvalues whose real part has the smallest modulus.

Tables I and II give the complex eigenvalues with positive real part and $0 \leqslant R \leqslant 100$ for odd and even eigenfunctions, respectively. The complex eigenvalues

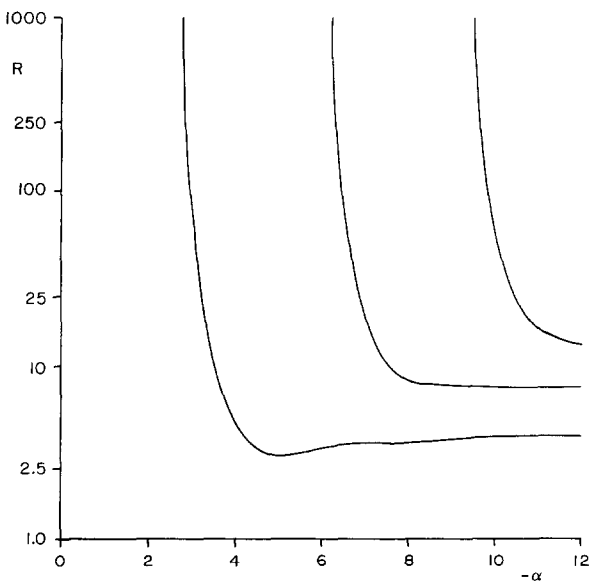

FIG. 5. Graph of negative real odd eigenvalues against Reynolds number.

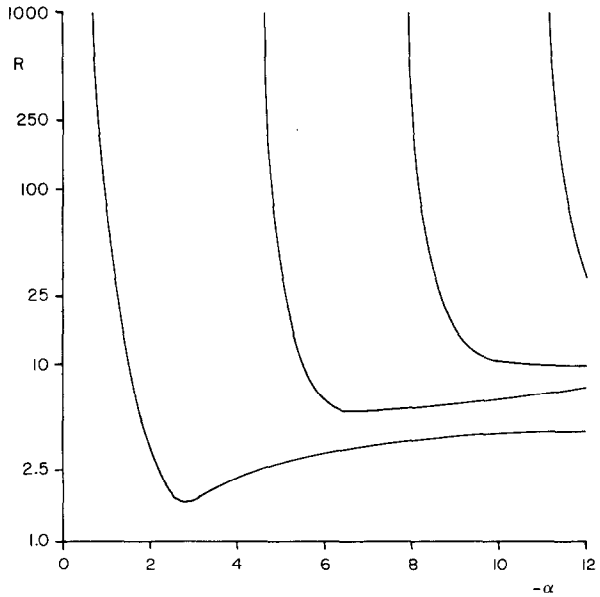

FIG. 6. Graph of negative real eigenvalues against Reynolds number.

occur in complex conjugate pairs but, as stated previously, only the one with positive imaginary part is given. A maximum of three odd and three even eigenvalues are given. Difficulty was encountered with the accuracy of the complex eigenvalues for R greater than 10. It was decided that it was not worthwhile increasing the number of Chebyshev polynomials in order to try to obtain these eigenvalues to greater accuracy. Tables III and IV give the complex eigenvalues with negative real part and $0 \leqslant R \leqslant 10$ for odd and even eigenfunctions, respectively. The real negative parts of these eigenvalues become larger in modulus and thus the associated disturbance will

TABLE I

Complex Odd Eigenvalues with Positive Real Part for $0 \leqslant R \leqslant 100$

R	Eigenvalues		
0	3.74884 + 1.38434i	6.94998 + 1.67611i	10.11926 + 1.85838i
0.25	3.67669 + 1.39141i	6.88416 + 1.67614i	10.05522 + 1.85719i
0.5	3.60752 + 1.39392i	6.81987 + 1.67224i	9.99225 + 1.85216i
1.0	3.47788 + 1.38708i	6.69588 + 1.65362i	9.86952 + 1.83117i
2.5	3.15444 + 1.29660i	6.36092 + 1.52056i	9.52773 + 1.68360i
5.0	2.80083 + 1.00736i	5.93589 + 1.00826i	9.067381 + 1.01552i
10.0	3.37037 + 0.51693i	6.53508 + 1.08843i	
25.0	2.66742 + 0.25719i	6.2473 + 0.8581i	
50.0	2.6942 + 0.2156i		
100.0	2.8245 + 0.4041i		

TABLE II

Complex Even Eigenvalues with Positive Real Part for $0 \leqslant R \leqslant 100$

R	Eigenvalues		
0	2.10620 + 1.12537i	5.35627 + 1.55157i	8.53668 + 1.77554i
0.25	2.02356 + 1.15434i	5.28839 + 1.55345i	8.47198 + 1.77476i
0.5	1.94628 + 1.17428i	5.22251 + 1.55126i	8.40853 + 1.77011i
1.0	1.80723 + 1.19347i	5.09672 + 1.53598i	8.28540 + 1.74994i
2.5	1.49815 + 1.15848i	4.76630 + 1.41771i	7.94678 + 1.60814i
5.0	1.22061 + 1.01508i	4.36877 + 1.00534i	7.50198 + 1.01230i
10.0	1.01976 + 0.77058i	4.97905 + 0.90975i	8.08350 + 1.20716i
25.0	1.0416 + 0.6093i	4.78856 + 0.72461i	7.7089 + 0.8531i
50.0	0.8780 + 0.5191i	4.5279 + 0.5966i	
100.0	0.8178 + 0.4577i	4.5752 + 0.4633i	

TABLE III

Complex Odd Eigenvalues with Negative Real Part for $0 \leqslant R \leqslant 10$

R	Eigenvalues		
0.25	−3.82402 + 1.37214i	−7.01732 + 1.67184i	−10.18436 + 1.85554i
0.5	−3.90229 + 1.35414i	−7.08617 + 1.66298i	−10.25051 + 1.84840i
1.0	−4.06847 + 1.29740i	−7.22828 + 1.62944i	−10.38594 + 1.81985i
2.5	−4.66051 + 0.81952i	−7.68379 + 1.32550i	−10.81542 + 1.56878i
5.0	−7.26515 + 1.25674i	−10.23210 + 1.24138i	−13.25578 + 1.26825i
10.0	−10.45868 + 1.69482i	−13.89801 + 1.34374i	−16.74203 + 1.38643i

TABLE IV

Complex Even Eigenvalues with Negative Real Part for $0 \leqslant R \leqslant 10$

R	Eigenvalues		
0.25	−2.194271 + 1.08519i	−5.42613 + 1.54525i	−8.60263 + 1.77221i
0.5	−2.28784 + 1.03093i	−5.49796 + 1.53398i	−8.66982 + 1.76447i
1.0	−2.49155 + 0.86105i	−5.64733 + 1.49407i	−8.80784 + 1.73410i
2.5	−6.11865 + 1.12698i	−9.24808 + 1.46334i	−12.38445 + 1.65452i
5.0	−6.40282 + 0.72826i	−8.77209 + 1.15148i	−11.73277 + 1.25837i
10.0	−10.15863 + 1.20719i	−15.23126 + 1.17982i	−18.19762 + 1.39851i

TABLE V

Eigenvalues for $R = 100$

Odd/Even	Eigenvalue α	Number of zeros in velocity	Odd/Even	Eigenvalue α	Number of zeros in velocity
Real positive			Real negative		
E	0.14540	1	E	−0.97667	1
O	0.18808	2	O	−2.99921	2
E	0.52747	3	E	−4.77226	3
O	0.57534	4	O	−6.48382	4
O	1.17751	6	E	−8.16908	5
E	1.40059	7	O	−9.84084	6
O	2.03429	6			
E	2.36435	9	Complex		
E	3.53450	7	E	0.81781 + 0.45772i	
O	3.97201	8	O	2.82446 + 0.40412i	

decay more quickly; for this reason the complex eigenvalues with negative real part are not tabulated for R greater than 10.

For $R = 100$, 250, 500, 1000, and 2000, the eigenvalues are given in Tables V–IX, respectively. As will be seen from Figs. 3–6, there will be at least five odd and five even eigenvalues which are real and positive and at least three odd and three even eigenvalues which are real and negative. Even though as R is increased, the number of real eigenvalues increases, only ten positive and six negative eigenvalues are given because the disturbances associated with the extra eigenvalues decay more quickly than those listed. Only one or two complex eigenvalues are given in each case.

TABLE VI

Eigenvalues for $R = 250$

Odd/Even	Eigenvalue α	Odd/Even	Eigenvalue α
Real positive		Real negative	
E	0.05787	E	−0.84183
O	0.07525	O	−2.89221
E	0.19745	E	−4.65001
O	0.23009	O	−6.34217
E	0.43773	E	−8.00625
O	0.46933	O	−9.65519
O	0.79389		
E	0.85178		
O	1.20545	Complex	
E	1.36827	E	0.72120 + 0.37929i

TABLE VII

Eigenvalues for $R = 500$

Odd/Even	Eigenvalue α	Odd/Even	Eigenvalue α
Real positive		Real negative	
E	0.028913	E	−0.75548
O	0.037627	O	−2.83090
E	0.097983	E	−4.58128
O	0.11505	O	−6.26383
E	0.21101	E	−7.91770
O	0.23460	O	−9.55615
E	0.37383		
O	0.39657		
O	0.60114	Complex	
E	0.60642	E	0.65637 + 0.33642i

The number of odd or even Chebyshev polynomials M used is either 20 or 24 for most of the Reynolds numbers, with $M = 16$ for the small Reynolds numbers. As mentioned above, difficulty is experienced with the accuracy of the complex eigenvalues for the larger Reynolds numbers. With $M = 24$, the computer programme is required to find the eigenvalues of a square matrix of order 100. Increasing M should give a more accurate answer, but at this stage increasing M does not increase the accuracy of the answer. In the calculation the eigenvalues with smallest modulus tend to be more accurate. As R increases, the modulus of the complex eigenvalues increases relative to the modulus of the real eigenvalues. As a result, the complex eigenvalues will be less accurate because the real eigenvalues with smaller modulus will have taken precedence. The inverse method is used to calculate the last decimal place of the real positive eigenvalues for $R = 2000$. The real negative eigenvalues are

TABLE VIII

Eigenvalues for $R = 1000$

Odd/Even	Eigenvalue α	Odd/Even	Eigenvalue α
Real positive		Real negative	
E	0.01445	E	−0.67978
O	0.01881	O	−2.78220
E	0.04890	E	−4.52729
O	0.05752	O	−6.20280
E	0.10469	E	−7.84929
O	0.11729	O	−9.48026
E	0.18249		
O	0.19825		
E	0.28384	Complex	
O	0.30044	E	0.5965 + 0.2995i

TABLE IX

Eigenvalues for $R = 2000$

Odd/Even	Eigenvalue α	Odd/Even	Eigenvalue α
Real positive		Real negative	
E	0.007227	E	−0.6129
O	0.009408	O	−2.7434
E	0.02444	E	−4.4846
O	0.02876	O	−6.1549
E	0.05225	E	−7.7958
O	0.05865	O	−9.4212
E	0.09077		
O	0.09912		
E	0.14018	Complex	
O	0.15021	E	0.5419 + 0.2680i

only given to four decimal places; the full problem results are doubtful in the fifth decimal place and the inverse problem was unable to do better than this. Here the reason for the inverse problem not being able to give the fifth decimal place is that the gradient of the curves in Figs. 5 and 6 is nearly vertical for large R.

The main disadvantage of the method we have used is that, particularly for the larger Reynolds numbers, spurious eigenvalues are calculated by the programme. When the number of Chebyshev polynomials is changed by 4, say, this spurious eigenvalue either changes wildly or disappears altogether. It is difficult to compare the results obtained for the same R but different M because the eigenvalues are calculated in a different order. Barratt and Sloan [1] used the above method and obtained one spurious eigenvalue per calculation. In our calculations there is never more than one spurious eigenvalue but its position can vary wildly. No attempt has been made to explain this phenomenon, but care must be taken to check the eigenvalues with a different value of M or check using a different method.

Wilson [12] did not present nearly as many results as are presented in this paper. In general, where the present paper and Wilson calculate comparable real eigenvalues, the two papers are in agreement. In the case of complex eigenvalues, the above results only agree with Wilson for $R = 0$. To be more specific, the results of the present paper agree with Table I ($R = 0$) and Table III and disagree with Tables I ($R \neq 0$), II, and IV, where the table numbers are those of Wilson [12]. Wilson uses a completely different method to solve the differential eigenvalue problems, and reasons for the disagreement cannot be given without reproducing that work.

7. Comparisons with Numerical Data

Dennis and Smith [2] obtained numerical solutions of the Navier–Stokes equations in the form (2.1) over a wide range of R for the case of flow along a two-dimensional

channel with a symmetrically placed constriction created by a sudden decrease in width. Equation (2.1) was written as two simultaneous equations by introducing the vorticity ζ defined by the equation

$$\nabla^2\psi = -\zeta, \tag{7.1}$$

and the two equations were solved numerically for ψ and ζ over the region of half the channel shown in Fig. 7. A steady Poiseuille velocity distribution was applied as a boundary condition both upstream and downstream, the upstream condition being

$$\psi \sim \tfrac{3}{2}y - \tfrac{1}{2}y^3, \qquad \zeta \sim 3y \qquad \text{as} \quad x \to -\infty, \tag{7.2}$$

and that downstream

$$\psi \sim 3y - 4y^3, \qquad \zeta \sim 24y \qquad \text{as} \quad x \to \infty. \tag{7.3}$$

The channel walls were located at $y = \pm 1$ upstream and $y = \pm\frac{1}{2}$ downstream, with $x = 0$ situated at the step discontinuity in width. In this problem, the flow is symmetrical about the centre line $y = 0$ and both ψ and ζ are therefore odd functions of y; thus only odd eigenfunctions will appear in the asymptotic expansions valid for large $|x|$.

For large enough distances upstream, the stream function ψ can be approximated by

$$\psi \sim \tfrac{3}{2}y - \tfrac{1}{2}y^3 + \sum_{n=1}^{\infty} f_n(y)\, e^{-\alpha_n x}, \tag{7.4}$$

where α_n are the appropriate eigenvalues defined earlier and $f_n(y)$ are the associated eigenfunctions. The appropriate eigenvalues are those which are real and negative or complex with negative real parts, since these give the correct decay of ψ to the Poiseuille flow as $x \to -\infty$. For the purpose of the subsequent discussion, we shall assume that complex terms have been omitted for the following reason: Comparisons between the numerical and theoretical results are made upstream for $R \geqslant 10$. For R as large as this, the asymptotic expansion is dominated by terms involving α_n which

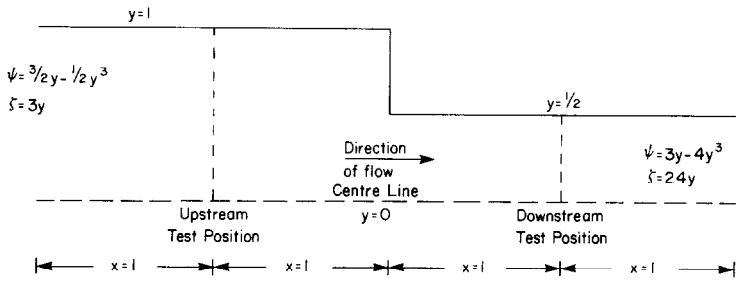

FIG. 7. Computational domain for Dennis and Smith [2].

are real. Therefore, there is no point in complicating the situation by introducing terms with complex α_n, since in all events we only require the first few terms. In the downstream direction, ψ can be approximated as $x \to \infty$ by

$$\psi \sim 3y - 4y^3 + \sum_{n=1}^{\infty} f_n^*(y)\, e^{-\alpha_n^* x}, \tag{7.5}$$

where the α_n^* are assumed to consist of only positive real eigenvalues with $f_n^*(y)$ the associated real eigenfunctions. Again the complex terms are omitted since comparisons downstream are made only for $R = 500$, for which the leading terms in (7.5) all have real positive α_n^*.

Far enough upstream, the summation in (7.4) will be dominated by the term associated with the smallest real negative eigenvalue, which is assumed to be α_1, and we easily deduce from (7.4) that

$$\frac{\partial \psi}{\partial x} \sim \alpha_1 \left(\frac{3}{2} y - \frac{1}{2} y^3 - \psi \right) \qquad \text{as} \quad x \to -\infty. \tag{7.6}$$

The comparable result downstream is

$$\frac{\partial \psi}{\partial x} \sim \alpha_1^* (3y - 4y^3 - \psi) \qquad \text{as} \quad x \to \infty, \tag{7.7}$$

where in this case α_1^* is the smallest positive real eigenvalue.

Equation (7.6) may be used in conjuction with the numerical solutions of Dennis and Smith [2] to obtain estimates of α_1 from the flow upstream of the step and Eq. (7.7) may similarly be used to estimate α_1^* from the flow downstream. Obviously, neither (7.6) nor (7.7) will give good approximations in the vicinity of the step. Moreover, they could not be applied near the upstream and downstream boundaries, respectively, used by Dennis and Smith in their numerical solutions since the Poiseuille velocity distribution was used as a boundary condition at these boundaries. For these reasons, stations were chosen to test the results (7.6) and (7.7) which were midway between the step and the respective upstream and downstream boundaries imposed in the numerical solutions; these are labelled the upstream and downstream test positions in Fig. 7. The comparisons of the present paper have been made with the numerical solutions of Dennis and Smith obtained using a grid size of $h = \frac{1}{40}$ for $R = 10$ and $h = \frac{1}{60}$ for $R > 10$, and with the upstream and downstream boundaries at $x = -2$ and $x = 2$. Thus the test positions are at $x = -1$ and $x = 1$, respectively.

Comparisons between the numerical results and the asymptotic results (7.6) can be made by estimating α_1 at given grid points from (7.6) using the numerical data for ψ and its derivative with respect to x. The results may then be compared with the calculated eigenvalue α_1. At the upstream test station an estimate of α_1 can be obtained for every grid point across the width of the channel. These estimates are then averaged to give a result which can be compared with the theoretical value of α_1 calculated in the present paper. This comparison is given in Table X. It indicates

TABLE X

Comparison Between the Present Calculation of the Theoretical Value of the Real Negative Eigenvalue with Smallest Modulus and the Estimate Obtained from the Numerical Solutions of Dennis and Smith [2]

R	10	50	100	500	1000	2000
Theoretical α_1	−3.528	−3.107	−2.999	−2.831	−2.782	−2.743
Estimated α_1	−3.526	−3.097	−2.984	−2.803	−2.737	−2.625

without doubt that the limiting flow upstream in this numerical example is described by the leading term of the theoretical asymptotic expansion associated with the negative eigenvalue α_1 of smallest magnitude. Similar results were obtained by making comparisons at stations situated quite a considerable distance either side of the upstream test station.

It is not possible to obtain a similar comparison between the present theory and the numerical results at the downstream test station for the smallest real positive eigenvalue. The main reason is that the real positive eigenvalues are much smaller and closer together and the smallest eigenvalue does not dominate downstream as the negative one of smallest modulus does upstream. It is of interest to note that Dennis and Smith [2] found in obtaining numerical solutions that, whereas it was relatively easy to resolve the situation of the flow upstream, the downstream calculations were much more difficult to resolve. There is a comparability of the situation in the present study; it is quite difficult to obtain an adequate check on the asymptotic nature of the flow downstream using the numerical data.

8. Summary and Discussion

In this paper the eigenvalues giving the perturbation from Poiseuille flow in a channel are calculated for a range of Reynolds numbers. The eigenvalues with positive real parts are associated with downstream disturbances ($x \to \infty$), while those with negative real parts are associated with upstream disturbances ($x \to -\infty$). The disturbances associated with the complex eigenvalues will be of an oscillatory nature, but in all cases it is the real part of the eigenvalue which is the factor that decides the rate of decay of the associated disturbances. There is little to be said about the rate of decay of the disturbances for small Reynolds numbers, but for larger values of R, the eigenvalues can be used to estimate the asymptotic departures from the parabolic profile. In general the eigenvalues associated with the upstream disturbances are an order of magnitude greater than the eigenvalues associated with the downstream disturbances. This implies that the upstream flow tends to the parabolic profile quicker than the downstream flow.

It may be possible to use the eigenvalues in the asymptotic boundary conditions for the numerical solution of flow in channels where the Poiseuille flow is assumed at

a large distance upstream or downstream, or both. In the upstream direction, the expansion can be taken in the form of Eq. (7.4) and in the downstream direction in the form of (7.5). The asymptotic conditions (7.6) and (7.7) can be deduced from these expansions, respectively, and it is these conditions which may be suitable for use as boundary conditions in numerical work. These equations have in fact been used to test the results of the present paper using the numerical solutions of Dennis and Smith [2]. The check is excellent upstream but unsatisfactory downstream. It is hoped to use the theoretical results of the present paper to develop boundary conditions suitable for use both upstream and downstream in future numerical work.

In checking the present results using the numerical solutions, we have utilized the fact that the eigenvalues which dominate the flow both upstream and downstream are real. The asymptotic formulation will be more complicated to use with oscillatory disturbances, but equally possible. For $R \geqslant 100$, upstream oscillatory disturbances are negligible and the upstream disturbances decay rapidly. For the downstream disturbances it is not until $R \geqslant 250$ that the oscillatory disturbances can be neglected.

This paper presents the eigenvalues of Eq. (2.6) subject to (2.7). The calculations are performed either from the full problem of determining the eigenvalues corresponding to a specified R or the inverse problem. Selected eigenfunctions have been calculated using the inverse problem rather than the full problem to save computer time. Some of the eigenvalue calculations agree with previous authors and some disagree. The real positive eigenvalues for large R tend to agree with the asymptotic form derived by Wilson [12] while the complex eigenvalues do not agree with his asymptotic form. One of the main contributions of the present paper is to study in detail the eigensolutions dominating the flow at large distances upstream with the associated more rapid decay rate.

ACKNOWLEDGMENT

J. S. Bramley is grateful to the Natural Sciences and Engineering Research Council of Canada for fincancial support during this study made while he was a visitor to the Department of Applied Mathematics at the University of Western Ontario.

REFERENCES

1. P. J. BARRATT AND D. M. SLOAN, *J. Fluid Mech.* **102** (1981), 389.
2. S. C. R. DENNIS AND F. T. SMITH, *Proc. R. Soc. London Ser. A* **372** (1980), 393.
3. L. FOX AND I. B. PARKER, "Chebyshev Polynomials in Numerical Analysis," Oxford Univ. Press, London/New York, 1968.
4. J. GILLIS AND A. BRANDT, AF EOAR 63-73 SR-1, Weizmann Institute, 1964.
5. C. LANCZOS, "Applied Analysis," Prentice–Hall, Englewood Cliffs, N.J., 1956.
6. C. L. LAWSON AND R. J. HANSON, "Solving Least Squares Problems," Prentice–Hall, Englewood Cliffs, N.J., 1974.
7. C. B. MOLER AND G. W. STEWART, *SIAM J. Numer. Anal.* **10** (1973), 241.
8. S. A. ORSZAG, *J. Fluid Mech.* **50** (1971), 689.

9. M. VAN DYKE, *J. Fluid Mech.* **44** (1970), 813.
10. J. H. WILKINSON, "The Algebraic Eigenvalue Problem," Clarendon, Oxford, 1965.
11. J. H. WILKINSON AND C. REINSCH, "Handbook for Automatic Computation, Linear Algebra," Vol. 2, p. 315, Springer-Verlag, New York/Berlin, 1971.
12. S. D. R. WILSON, *J. Fluid Mech.* **38** (1969), 793.
13. S. D. R. WILSON, *J. Fluid Mech.* **46** (1971), 787.